

## Simulation of a plasmonic tip-terminated scanning nanowire waveguide for molecular imaging

Nathan P. Malcolm,<sup>1</sup> Alex J. Heltzel,<sup>2</sup> Konstantin V. Sokolov,<sup>3</sup> Li Shi,<sup>1,a)</sup> and John R. Howell<sup>1,a)</sup>

<sup>1</sup>Department of Mechanical Engineering, The University of Texas at Austin, Austin, Texas 78712, USA

<sup>2</sup>PC Krause & Associates, West Lafayette, Indiana 47906, USA

<sup>3</sup>Department of Biomedical Engineering, The University of Texas M.D. Anderson Cancer Center, Houston, Texas 77030, USA

(Received 19 May 2008; accepted 14 October 2008; published online 10 November 2008)

Finite difference time domain simulation reveals plasmon coupling and local field enhancement at the gap between the gold nanoparticle (NP) tip of a ZnO nanowire (NW) waveguide and a gold-coated substrate or a gold NP probe. The region of field enhancement is about three times smaller than the 100 nm diameter of the gold NP tip, making the NW waveguide grown on a transparent microcantilever well-suited for near field imaging of single molecules immobilized on a gold substrate or gold NP-labeled cell membranes with superior spatial resolution and signal to noise ratio. © 2008 American Institute of Physics. [DOI: 10.1063/1.3013816]

Gold and silver nanoparticles (NPs) have been employed for surface-enhanced Raman scattering (SERS) and fluorescence (FL) spectroscopy of molecules, with enhancement factors of  $10^{14}$ – $10^{15}$  and  $10^{10}$  reported.<sup>1</sup> These large enhancement factors have drawn interest in the development of gold NPs as biological labels.<sup>2</sup> Individual gold NPs in live cells can be detected with optical techniques such as differential imaging contrast or confocal and dark-field optical microscopy.<sup>3</sup> However, resolving the spatial distribution of individual closely spaced Au NPs of sub-50 nm diameters remains a challenge for these far field optical techniques because of optical diffraction. Although far field optical nanoscopy such as stimulated emission depletion microscopy has beaten the diffraction limit, the smallest spot size achieved to date is still 62 nm.<sup>4</sup> On the other hand, electron microscopy (EM) can be used to resolve the spatial arrangement of gold NP labels on dried cells but not live cells. In addition, EM offers limited possibilities for simultaneous imaging of multiple target molecules.

Aperture near field scanning optical microscopy (NSOM) (Ref. 5) has overcome the optical diffraction limit. However, sub-50 nm aperture size is very difficult to obtain using the fiber pulling and metal coating processes and light transmission through the sub-wavelength aperture is very weak. On the other hand, the major drawback of the apertureless NSOM (ASNOM) method<sup>6</sup> is that the background noise can be much higher than the signal level, making it difficult to distinguish topographic artifacts from the actual signal. One approach to greatly improving the signal to noise ratio (SNR) of ANSOM is to employ two photon excitations of FL from a molecule.<sup>7</sup>

Recently, ZnO and SnO<sub>2</sub> nanowires (NWs) have been shown to be low-loss waveguides for ultraviolet and blue lights.<sup>8</sup> In a NW scanning microscopy method,<sup>9</sup> the second-order harmonic generation from an optically trapped KNbO<sub>3</sub> NW was used as a nanoscale light source for imaging. However, sub-50 nm spatial resolution was not demonstrated,

likely because light divergence from a NW light source makes the resolution not better than the NW diameter.

In this letter, we employ finite difference time domain (FDTD) simulation to investigate a molecular imaging method that employs plasmon coupling between the gold NP tip of a scanning ZnO NW waveguide and a gold substrate or a gold NP probe. Figure 1 illustrates the scanning NW waveguide that can be fabricated based on a wafer-stage process similar to that for batch fabrication of atomic force microscopy (AFM) probes with carbon nanotube tips.<sup>10</sup> The device contains a transparent SiN<sub>x</sub>/SiO<sub>2</sub> cantilever covered by a 50 nm thick metal film. A vapor-liquid-solid (VLS) transport process can be used to grow a ZnO NW at the end of the cantilever from a ~100 nm diameter opening patterned in the metal film. The obtained VLS ZnO NW is self-terminated with a gold catalytic NP at the free end.<sup>11</sup>

When a laser beam is focused through the transparent cantilever onto the junction between the ZnO NW and the cantilever, the metal film on the cantilever will block the laser beam except for that coupled into the ZnO NW. Our FDTD simulation shows that local electric field ( $E$ ) enhance-

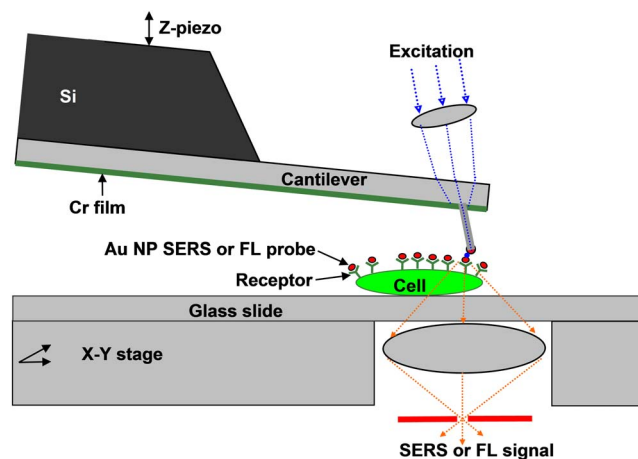


FIG. 1. (Color online) Schematic of the gold NP-terminated ZnO NW waveguide that is scanned on a cell membrane conjugated with gold NP SERS or FL probes.

<sup>a)</sup>Authors to whom correspondence should be addressed. Electronic addresses: lishi@mail.utexas.edu and jhowell@mail.utexas.edu.

ment occurs at the tip-sample gap when the gold NP tip of the NW is scanned on a gold substrate or a gold NP on a substrate. The region of field enhancement is about three times smaller than the 100 nm diameter of the tip, making the plasmon tip well suited for molecular imaging.

In a previous work, a three-dimensional FDTD program was developed to characterize the field enhancement due to laser-microsphere interaction.<sup>12</sup> This program is used in the current work to calculate the electric and magnetic field distributions at the ZnO NW tip. The program employs the Yee algorithm to solve for both electrical and magnetic field components in time and space.<sup>13</sup> An important aspect of a FDTD environment is the boundary condition. In order to prevent spurious reflection of electromagnetic waves at the edges of the simulation chamber, the convolution perfectly matched layer developed by Roden and Gedney<sup>14</sup> is used at all boundaries.

In the simulation, the top of a 202 nm thick SiO<sub>2</sub> cantilever is irradiated by a laser beam of uniform incident field intensity ( $E_i$ ) and wavelength ( $\lambda$ ) of 442 nm. This wavelength range avoids exciting photoluminescence that emits radially from the NW and is shorter than the wavelength with 50% intensity attenuation in the 100 nm diameter ZnO NW waveguide.<sup>15</sup> The cantilever is coated with 100 nm silver on the bottom surface except at the top of the NW. The NW is 1  $\mu$ m long and 100 nm in diameter, which is defined as that of the largest circle that can be fit within the hexagonal cross section of the NW. A hemispherical gold NP tip of diameter 100 nm is located at the free end of the NW. The cell size in the FDTD simulation is 2 nm by 2 nm by 2 nm, creating a simulation chamber with a total size of 1500  $\times$  600  $\times$  600 nm<sup>3</sup>. The total number of cells is about 67.5  $\times$  10<sup>6</sup>. The ZnO permittivity is taken as the bulk value of 10 $\epsilon_0$ ,<sup>16</sup> where  $\epsilon_0$  is the permittivity of vacuum. The permittivity and other Drude parameters for silver are compiled from Lynch and Hunter,<sup>17</sup> while the parameters for gold were compiled from Johnson and Christy.<sup>18</sup>

In one simulation shown in Fig. 2, the substrate is a 100 nm thick gold film that is separated from the gold NP tip by 8 nm. The angle ( $\theta$ ) between the NW axis and the normal of the Au substrate is varied between 0° and 60°. The laser polarization is parallel to the page, i.e.,  $p$ -polarization. The simulation reveals large local field enhancement at the tip-sample gap when  $\theta$  is between 7.5° and 30°, and little field enhancement when  $\theta$  is 0° or 45° [Fig. 2(c) and supplemental material].<sup>19</sup> The maximum field enhancement factor of about 29 is found at  $\theta=15^\circ$  [Fig. 2(a)], where the full width at half maximum (FWHM) of the enhanced  $E$  field spot on a plane 2 nm above the gold substrate is only about 34 nm [Fig. 2(b)]. The FWHM value is three times smaller than the NW diameter and about two times smaller than that reported for the bowtie aperture NSOM.<sup>20</sup>

The local  $E$  field enhancement is observed in the simulation only for  $p$  polarization and diminishes when the polarization is changed to  $s$  polarization that is perpendicular to the page (supplemental material).<sup>19</sup> Hence, it appears that the local field enhancement occurs when the laser polarization consists of a component parallel to the tip-sample gap. This finding is consistent with that of a reported study between two NWs, where localized plasmonic field enhancement was observed in the gap between the two NWs and dipolelike polarization charge distribution was found in each NW when

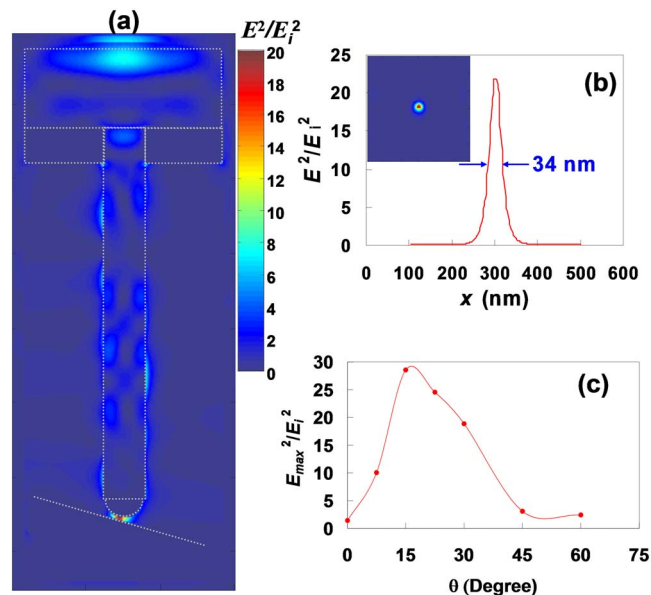


FIG. 2. (Color online) (a) Calculated electric ( $E$ ) field distribution on the NW central cross section plane when the gold NP tip of the ZnO NW is scanned at a distance of 8 nm above a gold substrate that is tilted from the horizontal by an angle  $\theta=15^\circ$ . The dashed lines are added to outline the 202 nm thick SiO<sub>2</sub> cantilever layer, 100 nm thick silver film, 100 nm diameter ZnO NW and gold NP tip, and the gold substrate surface. Image size: 600  $\times$  1500 nm<sup>2</sup>. (b)  $E$  field profile along a horizontal line passing the center of the bright spot shown in the inset. Inset:  $E$  field distribution on a plane 2 nm above the tilted gold substrate surface for the simulation result in (a). Image size: 600  $\times$  621 nm<sup>2</sup>. (c) The maximum  $E$  field ( $E_{max}$ ) at the tip-sample gap as a function of  $\theta$ . Symbols are the simulation results. The line is a least square fit of the symbols.

the polarization is parallel to the gap.<sup>21</sup> At  $\theta=0^\circ$  where the NW is perpendicular to the substrate, both the  $p$  and  $s$  polarizations are perpendicular to the vertical alignment of the tip-sample gap, so that little field enhancement results. However, it is unclear why the field enhancement diminishes for  $\theta$  at 45° or larger [Fig. 2(c)]. Nevertheless, the narrow  $\theta$  range that leads to large field enhancement results in the sub-50 nm FWHM.

In another simulation shown in Fig. 3, the sample is a 20 nm diameter gold NP on a glass slide. The angle ( $\theta$ ) between the NW axis and the normal of the glass slide is kept at 15°. The tip is scanned at a distance of 8 nm from the sample surface at the closest point. The horizontal distance ( $d_h$ ) between the center of the tip to the center of the NP is varied between -75 nm and 75 nm. Large local  $E$  field enhancement can be seen at the tip-sample gap when  $d_h$  is -62.5 and -50 nm [Fig. 3(a) and supplemental material].<sup>19</sup> Figure 3(b) shows the calculated maximum  $E$  field ( $E_{max}$ ) at the tip-sample gap as a function of  $d_h$ . For  $\lambda=442$  nm, the maximum enhancement factor of 7.5 occurs when  $d_h$  is -62.5 nm. The FWHM of the peak in the curve of Fig. 3(b) is 39 nm.

We have carried out additional simulations of three 20 nm diameter Au NPs on a glass slide tilted by 15 degrees from the horizontal. The results are shown in the supplemental material.<sup>19</sup> The empty gap between two adjacent Au NPs is 28 nm. When the NW tip scans across the sample with a fixed tip-sample distance of 8 nm, field enhancement is observed at the gap between the tip and only one of the three Au NPs when the NP is located at the left side of the NW axis and the horizontal distance between the center of the

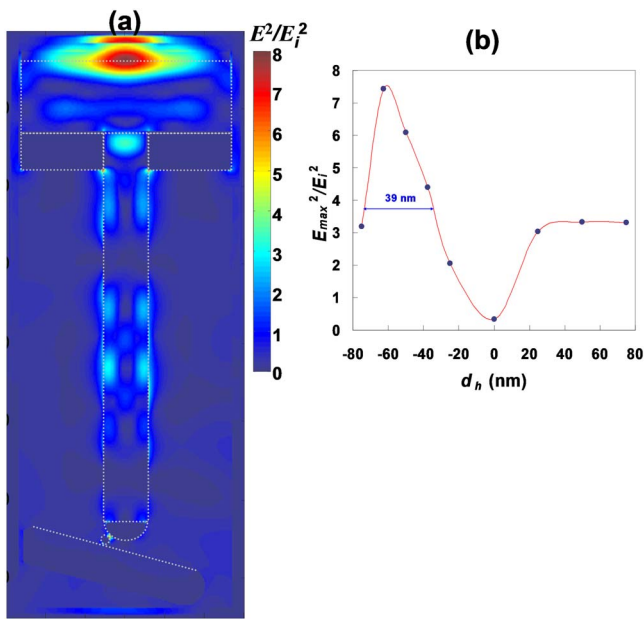


FIG. 3. (Color online) (a) FDTD simulation results of  $E$  field distribution on the NW central cross-section plane when the NW is scanned on a 20 nm gold NP on a glass slide, which is tilted from the horizontal by  $15^\circ$ . The horizontal distance ( $d_h$ ) between the tip center and the center of the 20 nm Au NP is  $-50$  nm. The dashed lines are added to outline the  $\text{SiO}_2$  cantilever layer, Ag film, ZnO NW and Au NP tip, the 20 nm diameter Au NP, and the surface of the glass slide. Image size:  $600 \times 1500$  nm $^2$ . (b) Maximum electric field ( $E_{\max}$ ) at the tip-NP gap as a function of  $d_h$ . Negative (or positive)  $d_h$  corresponds to the case when the 20 nm NP is at the left (or right) side of the tip in (a). Symbols are the simulation results. The line is a least square fit of the symbols.

particular NP and the NW axis is in the range between  $-37.5$  and  $-62.5$  nm. The field enhancement decays greatly when the tip is moved laterally by about 25 nm in either direction from the position where maximum enhancement is observed. In addition, we have also simulated an Au NP illuminated by a laser beam without the NW waveguide (see supplemental material).<sup>19</sup> The observed background intensity is higher than the case with the NW tip, as expected. Field enhancement is observed at the two sides of the NP, which is parallel to the horizontal polarization of the laser beam. This feature is apparently different from the case with the NW tip, where field enhancement occurs in the gap between the NP and the NW tip.

The plasmon coupling shown in the FDTD simulation is well suited for imaging molecules immobilized on a gold substrate or gold NP SERS or FL probes conjugated on a live cell membrane. For the latter case, plasmon coupling between the gold tip and a gold NP probe would excite SERS or FL from fluorescent or Raman tag molecules conjugated to a gold NP probe on a live cell membrane.<sup>22</sup> The highly localized field enhancement will address the major problem of very low transmission of round aperture NSOMs while obtaining sub-50 nm resolution. This feature will lead to improvement in both the spatial resolution and SNR compared to aperture NSOM. In addition, the simulation results show that the background illumination guided by the NW waveguide to the substrate surface is very weak and much lower than the micron-size intense laser beam focused on a metal tip of the ANSOM. Therefore, this method will greatly enhance the SNR compared to ANSOM. The SNR of the collected SERS or FL signals can be further enhanced by oscil-

lating the NP tip near the cantilever resonant frequency and measuring the corresponding oscillation amplitude of SERS or FL signals with lock-in amplifiers. Moreover, we note that this design can achieve resolution three times better than the NW diameter. This will be a great advantage compared to the recently reported NW scanning microscopy,<sup>9</sup> where the resolution is not better than the NW diameter. In addition, the high refractive index of the ZnO NW waveguide allows for tight light confinement even in liquid. This feature will allow for imaging of biologic cells and molecules in their natural liquid environment by using the gold tip-terminated NW waveguide operated in tapping mode AFM.<sup>23</sup> Nevertheless, the field enhancement depends sensitively on the tip-sample angle and gap, which will need to be adjusted carefully for the implementation of this design.

This work is supported in part by National Science Foundation (Grant No. CBET 0553649) and Texas Higher Education Coordinating Board Norman Hackerman Advanced Research Program. We thank Kort Travis for helpful comments on this manuscript.

- <sup>1</sup>S. M. Nie and S. R. Emery, *Science* **275**, 1102 (1997); J. B. Jackson and N. J. Halas, *Proc. Natl. Acad. Sci. U.S.A.* **101**, 17930 (2004).
- <sup>2</sup>P. Alivisatos, *Nat. Biotechnol.* **22**, 47 (2004); W. E. Doering, M. E. Piotti, M. J. Natan, and R. G. Freeman, *Adv. Mater. (Weinheim, Ger.)* **19**, 3100 (2007).
- <sup>3</sup>A. Kusumi, Y. Sako, and M. Yamamoto, *Biophys. J.* **65**, 2021 (1993); J. Aaron, E. de la Rosa, K. Travis, N. Harrison, J. Burt, M. Jose-Yacamán, and K. Sokolov, *Opt. Express* **16**, 2153 (2008).
- <sup>4</sup>V. Westphal, S. O. Rizzoli, M. A. Lauterbach, D. Kamin, R. Jahn, and S. W. Hell, *Science* **320**, 246 (2008).
- <sup>5</sup>E. Betzig, A. Lewis, A. Harootunian, M. Isaacson, and E. Kratschmer, *Biophys. J.* **49**, 269 (1986).
- <sup>6</sup>F. Zenhausern, M. P. Oboyle, and H. K. Wickramasinghe, *Appl. Phys. Lett.* **65**, 1623 (1994).
- <sup>7</sup>E. J. Sánchez, L. Novotny, and X. S. Xie, *Phys. Rev. Lett.* **82**, 4014 (1999).
- <sup>8</sup>J. C. Johnson, H. Q. Yan, P. D. Yang, and R. J. Saykally, *J. Phys. Chem. B* **107**, 8816 (2003).
- <sup>9</sup>Y. Nakayama, P. J. Pauzauskie, A. Radenovic, R. M. Onorato, R. J. Saykally, J. Liphardt, and P. D. Yang, *Nature (London)* **447**, 1098 (2007).
- <sup>10</sup>Q. Ye, A. M. Cassell, H. B. Liu, K. J. Chao, J. Han, and M. Meyyappan, *Nano Lett.* **4**, 1301 (2004).
- <sup>11</sup>M. H. Huang, Y. Y. Wu, H. Feick, N. Tran, E. Weber, and P. D. Yang, *Adv. Mater. (Weinheim, Ger.)* **13**, 113 (2001).
- <sup>12</sup>A. Heltzel, S. Theppakuttai, S. C. Chen, and J. R. Howell, *Nanotechnology* **19**, 025305 (2008).
- <sup>13</sup>K. S. Yee, *IEEE Trans. Antennas Propag.* **14**, 302 (1966).
- <sup>14</sup>J. A. Roden and S. D. Gedney, *Microwave Opt. Technol. Lett.* **27**, 334 (2000).
- <sup>15</sup>D. J. Sirbuly, M. Law, P. Pauzauskie, H. Q. Yan, A. V. Maslov, K. Knutson, C. Z. Ning, R. J. Saykally, and P. D. Yang, *Proc. Natl. Acad. Sci. U.S.A.* **102**, 7800 (2005).
- <sup>16</sup>S. L. Pinkett, W. D. Hunt, B. P. Barber, and P. L. Gammel, *Temperature Characteristics of ZnO-Based Thin Film Bulk Acoustic Wave Resonators* (2001 IEEE Ultrasonics Symposium, Atlanta, GA, 2001), p. 823.
- <sup>17</sup>E. D. Palik, *Handbook of Optical Constants of Solids* (Academic, Orlando, 1985).
- <sup>18</sup>P. B. Johnson and R. W. Christy, *Phys. Rev. B* **6**, 4370 (1972).
- <sup>19</sup>See EPAPS Document No. E-APPLAB-93-087844 for information consisting of five figures of detailed simulation results referenced in the paper. For more information on EPAPS, see <http://www.aip.org/pubservs/epaps.html>.
- <sup>20</sup>L. Wang and X. F. Xu, *Appl. Phys. Lett.* **90**, 261105 (2007).
- <sup>21</sup>J. P. Kottmann and O. J. F. Martin, *Opt. Express* **8**, 655 (2001).
- <sup>22</sup>K. Sokolov, M. Follen, J. Aaron, I. Pavlova, A. Malpica, R. Lotan, and R. Richards-Kortum, *Cancer Res.* **63**, 1999 (2003).
- <sup>23</sup>H. G. Hansma, J. Vesenka, C. Siegerist, G. Kelderman, H. Morrett, R. L. Sinsheimer, V. Elings, C. Bustamante, and P. K. Hansma, *Science* **256**, 1180 (1992).